Published in final edited form as:
Aging Cell. 2003 December ; 2(6): 305–318.

Fast anterograde transport of Herpes Simplex Virus: Role for the amyloid precursor protein of Alzheimer's disease

Prasanna Satpute-Krishnan[1,2], **Joseph A. DeGiorgis**[2,3], and **Elaine L. Bearer**[1,2]

[1]Department of Pathology and Laboratory Medicine, Brown University, Providence, RI 02912, USA

[2]Marine Biology Laboratory, Woods Hole, MA 02543, USA

[3]National Institute of Health, NINDS, Bethesda, MD 20892, USA

Summary

Anterograde transport of herpes simplex virus (HSV) from its site of synthesis in the neuronal cell body out the neuronal process to the mucosal membrane is crucial for transmission of the virus from one person to another, yet the molecular mechanism is not known. By injecting GFP-labeled HSV into the giant axon of the squid, we reconstitute fast anterograde transport of human HSV and use this as an assay to uncover the underlying molecular mechanism. HSV travels by fast axonal transport at velocities four-fold faster (0.9 μm/sec average, 1.2 μm/sec maximal) than that of mitochondria moving in the same axon (0.2 μm/sec) and ten-fold faster than negatively charged beads (0.08 μm/sec). Transport of HSV utilizes cellular transport mechanisms because it appears to be driven from inside cellular membranes as revealed by negative stain electron microscopy and by the association of TGN46, a component of the cellular secretory pathway, with GFP-labeled viral particles. Finally, we show that amyloid precursor protein (APP), a putative receptor for the microtubule motor, kinesin, is a major component of viral particles, at least as abundant as any viral encoded protein, while another putative motor receptor, JIP 1/2, is not detected. Conventional kinesin is also associated with viral particles. This work links fast anterograde transport of the common pathogen, HSV, with the neurodegenerative Alzheimer's disease. This novel connection should prompt new ideas for treatment and prevention strategies. Key words: Herpes Simplex Virus; HSV; amyloid precursor; protein; APP; kinesin; fast axonal transport; anterograde transport.

Introduction

Epidemiological evidence for a correlation between herpes simplex virus type 1 (HSV) and Alzheimer's disease has recently been accumulating (Jamieson *et al.*, 1991; Dobson & Itzhaki, 1999; Itzhaki & Dobson, 2002), although the molecular basis of this is unknown. During its life cycle, HSV travels into and out of the neuronal cell body within neuronal processes. Initially, HSV infects the mucosal membranes of the mouth or eye and secondarily enters sensory nerve terminals. After travelling within the neuronal process back to the cell body by retrograde transport (Topp *et al.*, 1994; Sodeik *et al.*, 1997; Bearer *et al.*, 2000; Dohner *et al.*, 2002), HSV either enters latency or replicates. Once replicated, newly

Correspondence: Elaine L. Bearer, MD/PhD, Department of Pathology and Laboratory Medicine, Biomedical Center Rm 518, Brown University Medical School, Providence, RI 02912, USA. Tel.: +1 401 863 3478; fax: +1 401 863 9008; Elaine_Bearer@Brown.edu.

Supplementary material

The movie clips referred to in Figs 2(A) and 3(A) can be viewed in full at http://www.blackwellpublishing.com/products/journals/suppmat/ACE/ACE069/ACE069sm.htm

synthesized HSV returns to the mucosal membrane, travelling out of the neuronal process apparently driven by fast anterograde transport (Lycke *et al.*, 1984; Kristensson *et al.*, 1986; Holland *et al.*, 1999; Miranda-Saksena *et al.*, 2000; Tomishima & Enquist, 2001; Enquist *et al.*, 2002; Willard, 2002). Returning virus re-infects the mucosal epithelium, causing the well-known recurrent herpetic sore that disseminates virus to new hosts (Roizman & Knipe, 2001; Whitley, 2001). This cycle of retrograde transport, latency, replication and anterograde transport has successfully propagated the virus such that ~51–80% of Americans are seropositive (Whitley, 2001; Xu *et al.*, 2002), yet the molecular mechanisms of transport remain undiscovered. Neither the viral proteins required nor the cellular machinery has been identified.

HSV is an enveloped DNA virus with four concentric compartments: a central DNA core within an icosahedral capsid encased in an amorphous tegument and enveloped in a glycoprotein-rich membrane (Roizman & Knipe, 2001). Enveloped virus is apparently assembled in the cytoplasm of infected cells. The viral glycoproteins of the envelope pass through the neuronal Golgi apparatus during synthesis (Johnson & Spear, 1982; Koga *et al.*, 1986; Whealy *et al.*, 1992; Miranda-Saksena *et al.*, 2000; Granzow *et al.*, 2001; Jensen & Norrild, 2002). The cytoplasmic tails of these viral glycoproteins serve as docking sites for tegumented capsids, which then bud into the lumen of Golgi-derived membrane compartments (Mettenleiter, 2002). Thus, inside cells some fully enveloped viral particles reside within Golgi-derived vesicles.

HSV does not encode its own motor, and therefore must recruit cellular motors either directly via a viral protein that binds motors, or indirectly by recruiting a motor receptor from the cell. Evidence exists for both types of motor recruitment (Miranda-Saksena *et al.*, 2000; Granzow *et al.*, 2001; Tomishima, 2001). Transport of HSV within a second, cellular membrane would be expected to occur according to normal cellular transport mechanisms that deliver post-Golgi secretory and synaptic vesicles to nerve termini. Such fast anterograde transport of membranated vesicles occurs in all neurons, where it mediates the rapid delivery of molecules synthesized and packaged in the Golgi apparatus of the neuronal cell body out long processes to the nerve termini. Fast anterograde transport plays a crucial role in neuronal functioning, being required for growth cone advance (Martenson *et al.*, 1993) and for maintenance and formation of the synapse (Goldstein & Yang, 2000). Vesicles to be transported apparently pick up motors by displaying motor receptors on their cytoplasmic surface as they exit the Golgi apparatus (Terada & Hirokawa, 2000; Kamal & Goldstein, 2002; Klopfenstein *et al.*, 2002). Thus, budding of HSV into post-Golgi membranes would place it in the right location to recruit these cellular motor receptors.

Amyloid precursor protein (APP) has been identified as a putative motor receptor (Kamal *et al.*, 2000, 2001). Proteolysis of APP is implicated in the pathogenesis of Alzheimer's disease (Beyreuther *et al.*, 1991; Price *et al.*, 1995; Neve *et al.*, 2000) and mutations in the human APP gene can lead to familial Alzheimer's disease (Price *et al.*, 1995; Sisodia & Price, 1995; Neve *et al.*, 2000; Selkoe, 2001; Evin & Weidemann, 2002). Fragments of APP accumulate at synapses and around neurons and are thought to be cytotoxic. The discovery that APP may play a role in transport has led to the resurgence of the hypothesis that the underlying defect in Alzheimer's disease is abnormal transport (Goldstein, 2001).

APP is a 695-kDa transmembrane protein with high amino acid sequence homology across species (Bayer *et al.*, 2001). *In vitro*, the 47 amino acid C-terminus cytoplasmic tail of APP binds to the tetratrico peptide motif of kinesin light chain, KLC1, and binding is required to produce a ternary complex with kinesin heavy chain, which contains the motor domain (Kamal *et al.*, 2000). Additional evidence suggests that this APP–kinesin association plays a functional role in anterograde transport. First, APP is transported in neurons. It accumulates

at sites of axonal damage in the brain and spinal cord in humans after head trauma (Gentleman *et al.*, 1993), as well as at the upstream side of a sciatic nerve ligation in an experimental mouse model (Kamal *et al.*, 2000, 2001). This accumulation is decreased in KLC1 knock-out mice (Kamal *et al.*, 2000). Second, APP and conventional kinesin heavy chain, KIF5a, co-purify with a subset of membrane-bound vesicles from the brain and sciatic nerve (Kamal *et al.*, 2001). Third, cleavage of APP liberates both its cytoplasmic tail and kinesin from transport vesicles (Kamal *et al.*, 2001). Finally, axonal transport is disrupted when the APP-like gene is deleted in *Drosophila* (Gunawardena & Goldstein, 2001). Thus APP binds kinesin *in vitro* and is itself transported *in vivo*, but whether APP is sufficient on its own to mediate transport is not yet known. APP is enriched in the Golgi network of mature neurons (Caporaso *et al.*, 1994) where it could encounter HSV during assembly.

The giant axon of the squid provides an assay for the molecular requirements of transport (Pant *et al.*, 1978; Allen *et al.*, 1982; Lasek & Brady, 1985; Vale *et al.*, 1985a,b; Kuznetsov *et al.*, 1992; Schnapp *et al.*, 1992; Bearer *et al.*, 1993, 1996a,b; DeGiorgis *et al.*, 2002). The molecular machinery for microtubule-based transport is highly conserved (Niclas *et al.*, 1994), allowing molecules from other species to be tested in this powerful model system (Schroer *et al.*, 1985). Endogenous transport vesicles in the axon move for up to 6 h after dissection, at average velocities of 2.15 $\mu m\ s^{-1}$ whereas larger particles, mostly mitochondria, move more slowly (Allen *et al.*, 1982; Vale *et al.*, 1985a). The large size of the axon allows injections of macro-molecular complexes, such as filamentous polymers of cytoskeletal proteins (Galbraith *et al.*, 1999) and even fluorescent beads as large as 1 μm in diameter (Terasaki *et al.*, 1995). Depending on their composition, injected particles may remain stationary or be actively transported in either the retrograde or the anterograde direction. Exogenous negatively charged particles injected into squid axons are transported in the anterograde direction very slowly (0.078 $\mu m\ s^{-1}$) (Terasaki *et al.*, 1995). Despite this non-specific transport the squid axon is useful as an assay for motor receptors. Not only is transport of negatively charged beads slow, but it is also rare (< 25% of beads move, even at sites distant from the injection where they had presumably arrived via transport). By contrast, HSV stripped of its envelope and injected into the axon travels rapidly (2.2 $\mu m\ s^{-1}$) in the opposite, retrograde, direction (Bearer *et al.*, 2000), demonstrating a specific, functional HSV–motor interaction in the squid axoplasm. Dynein and dynactin have now been shown to mediate the transport of incoming viral capsids to the nucleus of infected cells (Dohner *et al.*, 2002).

Here, we hypothesized that HSV recruits an anterograde motor, kinesin, from the host cell, in this case indirectly via the putative motor receptor, APP. We tested this by injecting green fluorescent protein (GFP)-labelled virus into the squid axon and observing its behaviour. Because stripped HSV was transported in the retrograde direction in squid axons, we reasoned that reconstitution of anterograde motility in squid would also be possible. We began our investigation by developing a procedure to obtain HSV that was motile in the anterograde direction when injected into the giant axon. Viral particles were labelled during assembly with GFP-VP16 for imaging by confocal microscopy after injection (Bearer *et al.*, 2000). To determine specificity of HSV transport, velocity and directionality of GFP-HSV were compared with those of endogenous mitochondria moving in the same axon. We then characterized the structure of motile virus by electron microscopy to determine whether it was encased in a second, Golgi-derived, membrane. Finally, we analysed the molecular composition of motile virus by Western blot and immunofluorescence to see which cellular proteins were associated with it. These studies identified APP as a major component of virus capable of anterograde motility. This demonstrates a surprising and novel molecular and physiological link between the common neuronal pathogen HSV and a common neurodegenerative disease, Alzheimer's disease.

Results

Anterograde transport of HSV in the giant axon of the squid

HSV labelled on tegument with VP16-GFP was harvested from infected cell cytoplasm, isolated by sucrose density gradient and injected into the giant axon of the squid. This allowed transfer of intracellular virus directly into the axon, bypassing all the steps normally involved in infection and viral replication. Immediately after injection, a plume of GFP-labelled viral particles appeared on the syneptic (anterograde) side of the injection site (Fig. 1), identified by two oil droplets. These droplets were co-injected on either side of the bolus of virus and remained stationary in healthy axons, thus serving as markers for the injection site as well as indicators of axonal integrity (Terasaki *et al.*, 1995).

Large numbers of GFP-labelled viral particles were transported in the anterograde direction (Fig. 2A). Adjacent stationary particles present at the injection site testify that this movement is specific and not the consequence of generalized axoplasmic streaming. At sites 1–5 mm towards the synapse, 96% of all particles moved continuously in the anterograde direction across the field. Neither a plume nor individual particles were observed on the retrograde side of the injection site facing towards the cell body. Tracings of viral movements demonstrated that some viral particles paused up to three times in a single 50-frame (138 s) sequence, whereas others displayed unidirectional continuous movement (Fig. 2B). Very short retrograde moves occurred during pauses, probably representing the recoil observed for endogenous particles (Allen *et al.*, 1982). A few (< 1%) of the injected particles travelled in the retrograde direction. These may represent tegument-exposed particles, because detergent-stripped HSV travels uniquely in the retrograde direction in squid axons (Bearer *et al.*, 2000).

To determine whether viral particles were moving according to a specific mechanism, we compared their transport with that of mitochondria in the same axon. Mitochondria are transported in squid slightly faster than negatively charged beads (Allen *et al.*, 1982; Vale *et al.*, 1985a; Terasaki *et al.*, 1995). Because mitochondria can be imaged with a cell-permeable dye, Rhodamine 123 (R123), their transport provides an internal monitor of the rates expected of exogenous particles without requiring additional injection. R123 is taken up by metabolically active mitochondria (Scaduto & Grotyohann, 1999), and therefore staining confirms axonal viability as well as transport.

Mitochondria, detected as R123-stained particles, were transported in both anterograde and retrograde directions (Fig. 3A). These mitochondria were imaged in the same axon as shown in Fig. 2. The lower speed of mitochondrial transport necessitated four-fold higher magnification and two-fold longer time-lapse intervals (5 s) than that for HSV transport, even when travelling in the same axon. Tracings of the tracks followed by mitochondria demonstrate bi-directionality with more frequent pauses than virus (Fig. 3B).

GFP-HSV travelled at average rates of $0.9 \pm 0.3\ \mu m\ s^{-1}$ ($n = 73$) with a maximum velocity for any single move of $1.23\ \mu m\ s^{-1}$ (Fig. 3C, grey bars). This is comparable with rates of fast anterograde transport of endogenous vesicles of similar size in the squid axon (Vale *et al.*, 1985a). By contrast, mitochondria travelled more slowly, at $0.2 \pm 0.08\ \mu m\ s^{-1}$ ($n = 45$) with a maximum velocity of $0.4\ \mu m\ s^{-1}$ (Fig. 3C, black bars). This difference in rates cannot be due to size difference, because membranated HSV and squid mitochondria are similar in size (0.23–0.44 μm and 0.2–0.5 μm in diameter, respectively). Furthermore, the size of negatively charged particles apparently does not affect their slow transport rate in squid axons–particles ranging from 20 nm to 0.5 μm are reportedly carried at similar, slow, rates in squid (Terasaki *et al.*, 1995). Thus, the faster transport of viral particles suggests a specific mechanism.

Rates of HSV transport were analysed by comparison with velocities of other types of transport cargo in invertebrate and vertebrate axons, including endogenous organelles such as mitochondria, and exogenous cargo such as nascent HSV synthesized in the cell and exogenously injected negatively charged beads (Table 1). This comparison demonstrates that HSV transport in squid is equivalent to reported rates for endogenous squid organelles in the 0.2–0.53 μm diameter size group (Table 1) (Allen *et al.*, 1982; Vale *et al.*, 1985a; Kamal *et al.*, 2000). Large negatively beads injected into crab axons move slightly faster than beads move squid (Adams & Bray, 1983), but these still move three-fold more slowly than the rate of HSV transport in squid.

Enveloped HSV inside a second membrane

Parallel aliquots of viral preparations with demonstrated motility were examined by negative stain electron microscopy (Fig. 4). These preparations contained three types of viral structures that could be readily distinguished by their size, contour and surface texture – capsids (icosahedral, 130 nm in diameter), and two species of membranated particles, one with a studded surface, 200–230 nm in diameter and the other with a smooth surface, 250–400 nm in diameter (Fig. 4A). Contours of both types of membranated particles revealed the presence of icosahedral capsids within. Capsids displayed the typical surface patterns of pentagons and triplexes previously described (Fig. 4B,B′) (Newcomb *et al.*, 1993), whereas the 200–230 nm membranated particles (71%, $n = 70$) displayed the more irregular studded surface typical of the viral envelope (Fig. 4C,C′) (Stannard *et al.*, 1987). By contrast, the larger membranated particles (29%) displayed smooth surfaces (Fig. 4D), but when broken open disclosed the studded surface of a viral envelope beneath (Fig. 4D′). Thus these larger particles probably represent virus that has budded into a second membrane, possibly derived from post-Golgi secretory vesicles.

To determine whether motile viral particles were associated with cellular Golgi-derived proteins, we used Western blotting followed by immunofluorescence. Immunofluorescence identified which viral particles were labelled with GFP and therefore confirmed association of cellular proteins with individual GFP-labelled virus. Because the evidence of motility was based on VP16-GFP fluorescence, only proteins associated with GFP-labelled particles can be considered candidates for motor recruitment. This eliminates the capsid, which although present in our preparation, does not include VP16 tegument and is therefore invisible in this assay.

HSV is associated with significant amounts of APP

To characterize the protein composition of viral particles, isolated virus was subjected to centrifugation to separate viral particles from soluble membranes and other proteins. Resultant supernatants and pellets were probed by Western blotting for viral and cellular proteins. To probe for APP, we used two anti-peptide antibodies, one raised against a domain in the lumenal/extracellular N-terminus and the other against the cytoplasmic C-terminus (Fig. 5). VP16-GFP together with proteins representing all three viral compartments (envelope, tegument and capsid) were detected exclusively in the pellet using antibodies against VP5 (capsid), VP22 (tegument), gD (envelope) and GFP (VP16-GFP) (Fig. 6A,B). This suggests that the viral particles we injected were intact, with no soluble component.

Cellular proteins also co-purified with virus. TGN46, a trans-membrane cellular protein known to be concentrated in the *trans*-Golgi network (TGN) (Prescott *et al.*, 1997), was detected exclusively in the viral pellets (Fig. 5B).

APP co-sedimented with motile viral particles, as demonstrated by re-probing blots with anti-peptide antibodies against either cytoplasmic domain of APP, C-APP (Fig. 6B) or the extra-cellular amino terminus domain, N-APP. Both of these anti-APP antibodies recognized a single band of ~120 kDa in pellets of isolated virus by Western blot. Antibodies directed against the amino terminus of APP, such as N-APP, should detect proteolytic products of APP. However, in five different viral preparations, no cleavage products of APP could be detected with either antibody, although the host cell is known to contain the proteolytic enzymes and to hydrolyse APP (Campadelli *et al.*, 1993; De Strooper *et al.*, 1995; Lo *et al.*, 1995; Caplan, 2001; Beher *et al.*, 2002). This suggests that HSV interferes with APP proteolysis.

Quantitative analysis of four separate viral preparations using these antibodies revealed that there were at least 10^3 molecules of APP per virion and possibly as many as 10^6. Thus, APP is at least as abundant as any viral protein, including gD and VP22 (Heine *et al.*, 1974; Haarr & Skulstad, 1994).

Viral particles were also probed for other cellular proteins, including conventional kinesin, synaptophysin, a synaptic vesicle marker, and JIP, another putative motor receptor (Fig. 6B) (Byrd *et al.*, 2001; Verhey *et al.*, 2001). Conventional kinesin was detected in viral pellets, albeit at low levels, and other kinesins, including Kif1a, were not found (data not shown). Kinesin associated with virus is unlikely to mediate transport in the squid axon, because the method for viral isolation involves steps likely to affect motor function. However, the presence of small amounts of this kinesin suggests it is the motor for viral transport, as would be expected because APP binds to its light chain (Kamal *et al.*, 2000). JIP was detected in cells but not in the viral preparation. JIP also interacts with APP (Byrd *et al.*, 2001; Matsuda *et al.*, 2001; Tarr *et al.*, 2002; Taru *et al.*, 2002) and may be associated with virus inside the cell, but cannot be responsible for the movements of isolated virus in the axon.

APP is physically associated with GFP-labelled motile HSV

To determine whether these cellular proteins were physically associated with GFP-labelled viral particles, parallel aliquots of virus from preparations with demonstrated motility in the axon were stained for viral and cellular proteins by indirect immunofluorescence. As expected, VP16-GFP-labelled particles stained for other viral components – capsid protein (VP5) and envelope glycoprotein (gD) (Fig. 6C). The staining patterns for each viral protein were morphologically appropriate, with anti-VP5 appearing as a capsid-like dot within or beside VP16-GFP-labelled tegument, and anti-gD surrounding the GFP, as expected for viral envelope.

More than half of the GFP-labelled viral particles also stained for the cellular protein, TGN46 (57%, $n = 168$) (Fig. 5C). TGN46 staining was not found independent of VP16-GFP. Of those GFP-labelled particles that also stained for TGN46, some (29%) were small vesicles containing a single particle, whereas the majority (71%) were larger sac-like membrane structures often containing multiple particles (Fig. 6C). These sac-like membranes resembled Golgi cisternae, complete with small peripheral buds. Aggregation of GFP-labelled particles in these sacs may explain why some were stationary at the injection site, as such aggregates would have difficulty moving through the dense axoplasm and such cisternae would not be expected to recruit motors. Indeed, groups of viral particles were never observed to move together.

Anti-C-APP stained the majority of VP16-GFP-labelled non-permeabilized particles (62% of all GFP-labelled viral particles, $n = 223$). Because anti-C-APP recognizes an epitope on the cytoplasmic surface of cellular vesicles (Dyrks *et al.*, 1988), this staining suggests that

the cytoplasmic tail is exposed on the surface of isolated viral particles. C-APP stained both small vesicles, containing a single GFP-labelled particle, or larger sacs with one or more particles. Significantly, many C-APP-stained vesicles were small with a single GFP-labelled particle (46% small vesicles and 54% sac-like, $n = 52$), a higher proportion than for TGN46 (Fig. 6C). The intensity of fluorescent staining for both TGN46 and APP was similar.

APP is removed together with anterograde motility

Anterograde motility is removed with detergent treatment (Bearer *et al.*, 2000). HSV that is detergent-extracted moves only retrogradely when injected into the giant axon. We therefore compared proteins present in intact or detergent-extracted viral particles to see if APP was removed (Fig. 6). Detergent extracted APP, as detected by both C- and N-APP antibodies, whereas tegument (VP22) and capsid (VP5) together with VP16-GFP were not extracted. Again, both C- and N-APP antibodies detected only a single, superimposable ~120-kDa band in viral preparations, with or without detergent treatment. The viral envelope (gD) as well as Golgi membrane marker (TGN46) were also extracted with detergent from viral particles. Thus, extraction of APP correlates with the loss of anterograde motility.

Discussion

Here we show that HSV harvested from infected cell cytoplasm is transported in the anterograde direction at fast transport rates up to 1.23 $\mu m\ s^{-1}$ when transferred by injection into the giant axon of the squid. These motile viral particles are associated with significant amounts of the cellular protein, APP, and some are encased in a second, possibly cellular, membrane. Only intact APP is detected associated with virus. Detergent treatment removes anterograde transport capability together with APP.

Although these studies do not directly address how HSV recruits APP, the second membrane surrounding viral particles appears to be derived from secretory vesicles arising from Golgi network where APP is also present (see Fig. 7). Thus, HSV recruits APP from the host cell, probably to mediate anterograde transport for egress. This recruitment may affect the location and extent of APP proteolysis and the consequent generation of the toxic Aβ fragment. Both derangement of transport and mislocalization of APP and its fragments may result in synaptic and neuronal dysfunction such as are seen in progressive Alzheimer's disease.

Transport of human HSV in the squid axon

There are several reasons to believe that the anterograde transport of HSV in the squid axon occurs according to normal physiological processes. (1) Retrograde transport of human HSV, stripped of envelope, occurs in squid by normal processes (Bearer *et al.*, 2000). (2) Like retrograde transport, the average rate for HSV anterograde transport (0.9 $\mu m\ s^{-1}$ up to a maximum of 1.2 $\mu m\ s^{-1}$) is comparable with the rate for endogenous squid vesicles of similar size in the axon (1.1 $\mu m\ s^{-1}$) (Vale, 1985a), and five- to ten-fold faster than the rate for mitochondria (0.2 $\mu m\ s^{-1}$) (Table 2). (3) The speed and sustained directionality of HSV transport relative to adjacent stationary objects further demonstrate that HSV transport is active and not a consequence of axoplasmic flow. (4) Anterograde velocity of HSV corresponds to transport rates of herpes virus in cultured vertebrate neurons, where the virus also moves faster than mitochondria, with virus labelled on the capsid travelling at 1.9 $\mu m\ s^{-1}$ (Smith *et al.*, 2001), and mitochondria at 0.24–0.41 $\mu m\ s^{-1}$ anterograde (Morris & Hollenbeck, 1993). (5) The linear and parallel tracks followed by VP16-GFP-labelled particles in the squid axon are reminiscent of the interwoven microtubule/actin bundles observed there by electron microscopy and confocal immunofluorescence imaging (Bearer

& Reese, 1999). Such filaments are known to serve as tracks for endogenous transport (Schnapp *et al.*, 1985; Vale, 1985; Signor & Scholey, 2000).

Motile HSV is associated with APP

The abundance of APP associated with viral particles argues that its association with HSV is physiological and necessary for function. APP is equivalent in abundance to the viral envelope glycoprotein, gD, with approximately 1000 copies per virion (Heine *et al.*, 1974). Such a large amount of APP is likely to be incorporated during intracellular packaging of the virus. APP localizes to the Golgi in uninfected cells and neurons (Caporaso *et al.*, 1994; Kaether *et al.*, 2000) and viral assembly is observed in the perinuclear and Golgi region of infected cells (Granzow *et al.*, 2001; Mettenleiter, 2002). Thus virus could recruit APP during passage through the Golgi. Our results are consistent with this; GFP-labelled viral particles were associated with TGN46, a protein found in the *trans*-Golgi network and in transport vesicles to and from the plasma membrane (Prescott *et al.*, 1997). In HSV-infected cells, TGN46 co-localizes with virus (McMillan & Johnson, 2001). Significantly, in cells infected with gI(−) HSV, TGN46 remains sequestered in the Golgi together with gE, another viral glycoprotein (McMillan & Johnson, 2001). This sequestration depends upon the cytoplasmic domain of gE. Together with our data, this implies that the viral glycoproteins, gI and gE, co-operate to recruit TGN46 during viral processing through the Golgi and this may also allow recruitment of APP along with Golgi membranes. Determination of interactions between TGN46 and APP will probably produce interesting information on how such recruitment occurs, not only for virus but for normal cellular transport as well.

The second membrane observed here surrounding viral envelopes probably corresponds to the outer membrane seen around intracellular enveloped virus in thin-section electron microscopy of alphaherpes viruses (Granzow *et al.*, 2001; Mettenleiter, 2002). The APP associated with our GFP-labelled virus is most likely present in this membrane as a normal component of the cellular Golgi-transport machinery. However, our experiments do not rule out the possibility that HSV recruits APP directly into its own envelope or that soluble viral structures bind APP as well. Furthermore, whereas APP is an abundant protein associated with virus and therefore is likely to play a major role in transport, it may not be the only motor receptor recruited by the virus. Our findings do not rule out the possibility that viral components might recruit motors by other mechanisms. Indeed, because synthesis of viral proteins requires trafficking through the cellular synthetic pathways, those motors involved in endoplasmic reticulum and Golgi motility are also likely to associate with viral components, and could possibly abnormally mediate axonal transport in infected cells. These motors include dyneins, KIF1c, and myosin V (Tabb *et al.*, 1998; Roghi *et al.*, 1999; Nakajima *et al.*, 2002; Wollert *et al.*, 2002). The unavoidable pleiomorphic characteristics of viral preparations would be expected to display all of these possibilities. In these studies we have focused only on APP, but additional mechanisms of transport, including other motor receptors as well as other motors, are also possible.

The motor

The motor driving transport of APP-associated virus is likely to be conventional kinesin. We detect small amounts of kinesin co-purifying with virus, and APP binds the tetratrico peptides in the kinesin light chain (Kamal *et al.*, 2000). Conventional kinesin, the first microtubule-based motor, was discovered in squid (Vale *et al.*, 1985) and subsequently found to be highly conserved across species (Goldstein & Yang, 2000; Miki *et al.*, 2001). In particular, the light chains of squid kinesin are homologous to mammalian kinesins (Beushausen *et al.*, 1993), and contain the tetratrico peptide domains that bind APP (Gindhart & Goldstein, 1996). The kinesins are now recognized to be a large family of

microtubule-based motor proteins (Miki *et al.*, 2001). No kinesins other than conventional kinesin have been identified in squid.

The high amino acid conservation of APP and of both heavy and light chains of conventional kinesin argues that the vertebrate homologue could interact with the squid kinesin. We therefore propose that the C-terminus of the cellular motor receptor, APP, displayed on the surface of injected viral particles, recruits conventional kinesin from squid for transport in the giant axon. These results do not prove that HSV inside cells exclusively recruits conventional kinesin. Other kinesins not present in squid may also contribute to intracellular viral motility.

Interaction between APP and kinesin could be direct or indirect via intermediaries. One candidate for this intermediary is JIP. The cytoplasmic domain of APP contains a highly conserved motif, GYENPTY, which binds JIP (Matsuda *et al.*, 2001; Taru *et al.*, 2002). JIP also binds the tetratrico motifs in kinesin light chain (Verhey *et al.*, 2001). JIP is a peripheral membrane scaffolding protein known to be transported (Bowman *et al.*, 2000; Byrd *et al.*, 2001; Verhey *et al.*, 2001) but whose membrane receptor is not known. APP could serve as the membrane receptor both for JIP and for kinesin. In this scenario, APP would recruit kinesin both directly and indirectly. Binding to the cytoplasmic domain of APP by kinesin, JIP or other proteins such as Shc (Tarr *et al.*, 2002) could protect APP from the proteolytic processing that produces the toxic Aβ fragment of Alzheimer's disease (Taru *et al.*, 2002). Kinesin dissociates from transport vesicles when APP is hydrolysed by gamma secretase (Kamal *et al.*, 2001), the enzyme thought to produce Aβ but whether dissociation is the cause or the effect of proteolysis is not clear. Indeed, where APP hydrolysis occurs inside the cell and how proteolysis is regulated are areas of vigorous inquiry, and will be important for viral transport as well. Although JIP is not detected on the viral particles, JIP is a highly conserved protein and is also likely to be present in the squid axon.

HSV may have or recruit additional factor(s) that promote and/or sustain motility. Other domains in the full-length cytoplasmic tail of APP may sustain kinesin attachment or may recruit other motors. This would include the juxtamembrane domain, which contains tyrosine phosphorylation sites that bind PAT1 (Zheng *et al.*, 1998). PAT1 binds microtubules and has sequence homology with KLC, suggesting that it may bind kinesin heavy chain. Virus may also sustain motility by recruiting more than one type of motor, such as actin-based motors. Indeed, actin-based motors may be required for transported virus to travel from the end of one microtubule to the next, which is hypothesized to occur on actin filaments (Kuznetsov *et al.*, 1992; Bearer & Reese, 1999). Actin-based motors are also present in the axon (Bearer *et al.*, 1993, 1996a,b; Langford *et al.*, 1994; Tabb *et al.*, 1998; Molyneaux *et al.*, 2000; Cohen, 2001; DeGiorgis *et al.*, 2002), and isolated axoplasmic organelles move on actin-filaments *in vitro* (Kuznetsov *et al.*, 1992; Bearer *et al.*, 1993, 1996a,b). Both myosin V and myosin II are found on the surfaces of axoplasmic organelles (Kuznetsov *et al.*, 1992; Bearer *et al.*, 1993, 1996a,b; Molyneaux & Langford, 1997; Tabb *et al.*, 1998; Cohen, 2001; DeGiorgis *et al.*, 2002). Myosin II has also been implicated in HSV egress via interaction with VP22 (van Leeuwen *et al.*, 2002). The collaboration of a variety of motor receptors and their motors is probably responsible for the inexorable delivery of virus to the mucosal membrane, a critical process in transmission, and thereby in long-term survival of the virus.

HSV and Alzheimer's disease

Association of HSV with APP raises questions about whether this interaction might be involved in the pathogenesis of Alzheimer's disease (AD). HSV DNA is detected in brains of patients with AD, suggesting a causal relationship (Jamieson *et al.*, 1991; Itzhaki *et al.*, 1997; Pyles, 2001; Grant *et al.*, 2002; Hemling *et al.*, 2003). ApoE4, an AD susceptibility

allele of the lipoprotein, ApoE (Selkoe, 2001), has been explored as a risk factor for HSV re-activation in AD (Itzhaki *et al.*, 1997; Itzhaki & Dobson, 2002). Plasma ApoE binds the HSV envelope glycoprotein, gB, and thereby could increase haematogenous dissemination of virus within the brain (Huemer *et al.*, 1988; Burgos *et al.*, 2002). It will be of interest to determine whether ApoE and APP are part of a single pathway in AD pathogenesis and how this pathway is affected by HSV. There are several ways that APP and ApoE interact. ApoE is present in amyloid plaques composed of the Aβ fragment of APP, and the ApoE4 isoform enhances plaque formation (Holtzman *et al.*, 2000). The receptor for ApoE, LPR, mediates endocytosis of secreted APP, and also binds the cytoplasmic domain of APP, which affects its proteolysis (Kounnas *et al.*, 1995; Pietrzik *et al.*, 2002).

Our findings that HSV interacts with APP provide an alternative hypothesis for the relationship between HSV and AD. The role of APP in transport has raised the intriguing possibility that transport defects may provide a pathogenic basis of AD (Goldstein, 2001). Disturbance of anterograde transport by HSV could well lead to abnormal location, accumulation and processing of APP in neurons, as well as of other proteins required for synapse maintenance and function. Abnormal accumulation of Aβ at the synapse could be further enhanced if processing of APP by LPR was differentially affected by the ApoE4 isoform.

Experimental procedures

Generation of GFP-labelled HSV

HSV was labelled with VP16-GFP as previously described (Bearer *et al.*, 2000). Vero cells plated in T175 flasks were transfected with pVP16-GFP and then infected by adding HSV1 strain hrR3 (Goldstein & Weller, 1988) at 1 MOI into 25 mL of the media. After 16 h, the Vero cells were scraped into media (25 mL), transferred to Falcon® tubes and frozen at − 80 °C. After thawing, the viral suspension was sonicated for 45 s at the 3rd setting with the Sonic Dismembranator (Fisher Scientific) and centrifuged for 10 min at 2000 ***g*** in the IEC cellfuge. The supernatant was filtered through a 0.8-μm Millipore® filter, and layered over a 15-mL three-step sucrose gradient of 60%, 30% and 10% (Beckman), and centrifuged for 2 h, at 80 000 × g, in the SW28 rotor. The lower band at the 60% sucrose interface was removed, the sucrose diluted and the virus collected for 1.5 h at 25 000 r.p.m. in the SW28 rotor. The resultant ~50-μL pellets were resuspended in 200 μL of PBS, yielding viral preparations of 1–5 × 10^9 viral particles mL^{-1}, which were aliquoted and stored at −80 °C. Parallel aliquots were analysed for motility, for structure by electron microscopy, and for protein composition by Western blots and immunofluorescence.

Dissection and microinjection of the giant axon of the squid

Giant axons were dissected from squid (*Loligo pealleii*) in Ca^{2+}-free seawater. Micropipettes were front-loaded with ~1500 pL of viral preparation at 10^9 viral particles mL^{-1} or ~1500 pL of peptide conjugated-fluorescent beads at 1.4 × 10^{12} beads mL^{-1}. In the case of peptide-conjugated beads, equal volumes of red and green fluorescent beads (1 : 1 suspension) were co-injected either after mixing or with one or the other colour loaded first. Micropipettes were capped at both sides of the injectate with dimethylpolysiloxane oil, which was co-injected with virus or beads and served as a stable marker of the injection site. General details for microinjection are available from Rindy Jaffe Microinjection Manual (http://155.37.3.143/panda/injection/).

After injection, axons were transferred to a chamber containing Ca^{2+}-free seawater that was designed for observation on the confocal microscope. In select axons, mitochondria were also stained by adding R123, at 2 μg mL^{-1} (Molecular Probes), into the surrounding

seawater. Penetration of R123 into the axon is slow, taking up to 2 h before mitochondria are easily visible. Transport in the axon will continue for over 4 h after dissection. Viability of axons was monitored at each step by observing the stability of oil droplets, staining and motility of mitochondria, and continued transparency of the axoplasm.

Imaging axonal transport by confocal microscopy

Movements of GFP-HSV or R123-stained mitochondria in the giant axon were collected on either a Bio-Rad 600 or Zeiss LSM 510 Laser Scanning Confocal Microscope with 10× plan neofluor 0.3 NA Air, and 40× Achroplan 0.8 NA Water Correctible objectives. Fluorescence and phase images were collected simultaneously using the multitracking option on the Zeiss LSM510. Images were collected at time intervals ranging from 1 to 10 s, with four-frame averaging for time intervals of 4 s or greater. The argon laser (488 nm) was used to excite the GFP and green fluorescent microspheres or the helium–neon laser (543 nm) for R123.

Analysis of transport

Rates and trajectories of VP16-GFP-HSV and mitochondria were measured by stepping through the frames in either the Zeiss LSM browser or NIH Image (http://rsb.info.nih.gov/nih-image/). Only particles moving into and out of a frame were included. Rates of moving particles were statistically analysed and plotted graphically using Kaleidagraph (Synergy Software).

Negative stain

For negative stain electron microscopy, virus was mounted on carbon-Formvar-coated EM grids and stained with 1% aqueous uranyl acetate (Bearer *et al.*, 2000). Grid squares with even distribution of viral particles and stain were selected and photographed at higher magnification at random. Particles in each micrograph were counted and categorized.

Western blot

Antibodies included mouse anti-VP5 (Virusys), mouse anti-VP22 (Invitrogen), mouse anti-gD (QED Biosciences), sheep anti-TGN46 (Serotec), mouse anti-kinesin (SUK4, Cytoskeleton), anti-squid kinesin (Chemicon), anti-synaptophysin (Sigma), mouse anti-GFP (Clontech), rabbit anti-C-APP (Zymed) and goat anti-N-APP (BioDesign).

An aliquot (20 μL) of motile virus was divided into two tubes. One was treated with 0.1% Triton-X100 in 0.6 M KCl for 30 min, 4 °C, and both treated and untreated were centrifuged in parallel at 100 000 ***g*** for 30 min. The resultant supernatants and pellets were separated and subjected to quantitative SDS gel electrophoresis, then immunoblotted. Blots were blocked in 1× TBS and 3.0% instant milk, incubated with primary antibody for 1.5 h, washed, and stained with horseradish-peroxidase-conjugated secondary antibody (Chemicon) for 20 min. Blots were washed and developed for ECL chemiluminescence (Amersham). Blots were stripped with 62.5 mM Tris-HCl, pH 6.8, 3.0% SDS, 50 mM 1,4 dithiothrietol, and reprobed. To compare the relative amounts of gD and C-APP, specific primary antibodies with similar sensitivities were used on the same blot at the same dilution, timing of incubations and film exposure. All antibodies were diluted in 1× TBS with 0.2% Tween + 3.0% milk.

For quantification of APP, densitometry of ECL Western blots was used to compare viral preparations with known amounts of synthetic APP peptides (sequences are shown in Table 1). Jumbled peptide was used as a control. Lanes containing viral preparations (5, 10 and 20 μL) were transferred from SDS-gels and probed in parallel on the same blot with series of dots containing either C- or N-APP peptides (10, 50, 100, 500 pg and 10, 50, 100, 500 ng).

A standard curve for each blot was generated based on the density of staining of the peptide dots determined by NIH image 1.62 of digitized blots. The density of the ~120-kDa band in the viral lanes was compared with the standard curve. Concentrations of viral particles were based on negative stain electron microscopy and HSV titres. Four different viral preparations and two different antibody–peptide combinations were analysed. The APP band was consistently equivalent to the 10-ng peptide dot in 20 μL of virus (10^9 particles mL^{-1}, ~50% membranated).

Immunofluorescence

VP16-GFP-HSV was diluted 1 : 20 in PBS, and 3 μL was applied to VWR® Superfrost® Plus microscope slides (VWR) and allowed to adhere for 5 min, then gently rinsed with PBS. For C-APP, VP22 and VP5 staining, GFP-HSV were neither fixed nor exposed to detergent and all incubations were with PB (PBS with 1% bovine albumin). For TGN46 and gD staining, viral particles were fixed with 4% paraformaldehyde and 0.25% Triton-X in PHEM buffer (60 mM PIPES pH 6.9, 25 mM HEPES pH 6.9, 10 mM EGTA, 2 mM $MgCl_2$). Subsequent incubations were performed in PBT (PB with 0.1% Triton-X100). After blocking, slides were incubated with Cy3-conjugated secondary (Jackson ImmunoResearch) and mounted in antiquench (1 mg mL^{-1} 4-diazabicyclo [2,2,]-octane (Sigma) in 90% glycerol : 10% PBS). Negative controls lacking the primary antibody were run in parallel. Randomly selected fields were collected on a Nikon fluorescence microscope equipped with the RT-Spot liquid crystal digital camera (Diagnostic Instruments) and a double rhodamine/fluorescein filter cube (Omega).

Sequence analysis

Primary sequence similarity search of the non-redundant (nr) database was performed using the PAM30 matrix without low-complexity filter, with expect at 20 000 and word size 2, in the basic, local alignment search tool (http://www.ncbi.nlm.nih.gov/BLAST).

Supplementary Material

Refer to Web version on PubMed Central for supplementary material.

Acknowledgments

We are grateful to Thomas S. Reese for his support, insightful comments and encouragement. Bearer laboratory members who contributed technical assistance include Paulette Ferland, Michael Conely, Paul Silva, Marcus Jang, Jamunabai Prakash, Zach Ginsberg, Jonathan Greer and Michelle Schlieff. We appreciate the technical advice of Jennifer LaVail, Jim Galbraith, Jennifer Petersen and Mark Terasaki. We thank Xandra O. Breakefield, Deb Schuback and Paola Grandi for the VP16-GFP-labelled HSV, and advice. The literature on APP, HSV and axoplasmic transport is extensive. We apologize to all those whose work we have not cited. Supported by NIH GMS 47562 (E.L.B.), NINDS (J.A.D. and T.S.R.) and the MCB NIH training grant (P.S.-K. and J.A.D.) Brown University.

References

Adams RJ, Bray D. Rapid transport of foreign particles microinjected into crab axons. Nature. 1983; 303:718–720. [PubMed: 6190095]

Allen RD, Metuzals J, Tasaki I, Brady ST, Gilbert SP. Fast axonal transport in squid giant axon. Science. 1982; 218:1127–1129. [PubMed: 6183744]

Bayer TA, Wirths O, Majtenyi K, Hartmann T, Multhaup G, Beyreuther K, Czech C. Key factors in Alzheimer's disease: beta-amyloid precursor protein processing, metabolism and intraneuronal transport. Brain Pathol. 2001; 11:1–11. [PubMed: 11145195]

Bearer EL, Breakefield XO, Schuback D, Reese TS, LaVail JH. Retrograde axonal transport of herpes simplex virus: evidence for a single mechanism and a role for tegument. Proc Natl Acad Sci USA. 2000; 97:8146–8150. [PubMed: 10884436]

Bearer EL, DeGiorgis JA, Bodner RA, Kao AW, Reese TS. Evidence for myosin motors on organelles in squid axoplasm. Proc Natl Acad Sci USA. 1993; 90:11252–11256. [PubMed: 8248236]

Bearer EL, DeGiorgis JA, Jaffe H, Medeiros NA, Reese TS. An axoplasmic myosin with a calmodulin-like light chain. Proc Natl Acad Sci USA. 1996a; 93:6064–6068. [PubMed: 8650220]

Bearer EL, DeGiorgis JA, Medeiros NA, Reese TS. Actin-based motility of isolated axoplasmic organelles. Cell Motil Cytoskel. 1996b; 33:106–114.

Bearer EL, Reese TS. Association of actin filaments with axonal microtubule tracts. J Neurocytol. 1999; 28:85–98. [PubMed: 10590510]

Beher D, Wrigley JD, Owens AP, Shearman MS. Generation of C-terminally truncated amyloid-beta peptides is dependent on gamma-secretase activity. J Neurochem. 2002; 82:563–575. [PubMed: 12153480]

Beushausen S, Kladakis A, Jaffe H. Kinesin light chains: identification and characterization of a family of proteins from the optic lobe of the squid Loligo pealii. DNA Cell Biol. 1993; 12:901–909. [PubMed: 8274223]

Beyreuther K, Bush AI, Dyrks T, Hilbich C, Konig G, Monning U, Multhaup G, Prior R, Rumble B, Schubert W, et al. Mechanisms of amyloid deposition in Alzheimer's disease. Ann NY Acad Sci. 1991; 640:129–139. [PubMed: 1776729]

Bowman AB, Kamal A, Ritchings BW, Philp AV, McGrail M, Gindhart JG, Goldstein LS. Kinesin-dependent axonal transport is mediated by the sunday driver (SYD) protein. Cell. 2000; 103:583–594. [PubMed: 11106729]

Burgos JS, Ramirez C, Sastre I, Bullido MJ, Valdivieso F, Selkoe DJ. Involvement of apolipoprotein E in the hematogenous route of herpes simplex virus type 1 to the central nervous system. J Virol. 2002; 76:12394–12398. [PubMed: 12414984]

Byrd DT, Kawasaki M, Walcoff M, Hisamoto N, Matsumoto K, Jin Y. UNC-16, a JNK-signaling scaffold protein, regulates vesicle transport in *C. elegans*. Neuron. 2001; 32:787–800. [PubMed: 11738026]

Campadelli G, Brandimarti R, Di Lazzaro C, Ward PL, Roizman B, Torrisi MR. Fragmentation and dispersal of Golgi proteins and redistribution of glycoproteins and glycolipids processed through the Golgi apparatus after infection with herpes simplex virus 1. Proc Natl Acad Sci USA. 1993; 90:2798–2802. [PubMed: 8385343]

Caplan MJ. Ion pump sorting in polarized renal epithelial cells. Kidney Int. 2001; 60:427–430. [PubMed: 11473621]

Caporaso GL, Takei K, Gandy SE, Matteoli M, Mundigl O, Greengard P, De Camilli P. Morphologic and biochemical analysis of the intracellular trafficking of the Alzheimer beta/A4 amyloid precursor protein. J Neurosci. 1994; 14:3122–3138. [PubMed: 8182461]

Cohen DL. Squid p196, a new member of the myosin-V class of motor proteins, is associated with motile axoplasmic organelles. Brain Res. 2001; 890:233–245. [PubMed: 11164789]

De Strooper B, Craessaerts K, Dewachter I, Moechars D, Greenberg B, Van Leuven F, Van den Berghe H, Wall JS, Brown JC. Basolateral secretion of amyloid precursor protein in Madin-Darby canine kidney cells is disturbed by alterations of intracellular pH and by introducing a mutation associated with familial Alzheimer's disease. J Biol Chem. 1995; 270:4058–4065. [PubMed: 7876155]

DeGiorgis JA, Reese TS, Bearer EL. Association of a nonmuscle myosin II with axoplasmic organelles. Mol Biol Cell. 2002; 13:1046–1057. [PubMed: 11907281]

Dobson CB, Itzhaki RF. Herpes simplex virus type 1 and Alzheimer's disease. Neurobiol Aging. 1999; 20:457–465. [PubMed: 10604441]

Dohner K, Wolfstein A, Prank U, Echeverri C, Dujardin D, Vallee R, Sodeik B. Function of dynein and dynactin in herpes simplex virus capsid transport. Mol Biol Cell. 2002; 13:2795–2809. [PubMed: 12181347]

Dyrks T, Weidemann A, Multhaup G, Salbaum JM, Lemaire HG, Kang J, Muller-Hill B, Masters CL, Beyreuther K. Identification, trans-membrane orientation and biogenesis of the amyloid A4 precursor of Alzheimer's disease. EMBO J. 1988; 7:949–957. [PubMed: 2900137]

Enquist LW, Tomishima MJ, Gross S, Smith GA. Directional spread of an alpha-herpesvirus in the nervous system. Vet Microbiol. 2002; 86:5–16. [PubMed: 11888685]

Evin G, Weidemann A. Biogenesis and metabolism of Alzheimer's disease Abeta amyloid peptides. Peptides. 2002; 23:1285–1297. [PubMed: 12128085]

Galbraith JA, Reese TS, Schlief ML, Gallant PE. Slow transport of unpolymerized tubulin and polymerized neurofilament in the squid giant axon. Proc Natl Acad Sci USA. 1999; 96:11589–11594. [PubMed: 10500221]

Gentleman SM, Nash MJ, Sweeting CJ, Graham DI, Roberts GW. Beta-amyloid precursor protein (beta APP) as a marker for axonal injury after head injury. Neurosci Lett. 1993; 160:139–144. [PubMed: 8247344]

Gindhart JG Jr, Goldstein LS. Tetratrico peptide repeats are present in the kinesin light chain. Trends Biochem Sci. 1996; 21:52–53. [PubMed: 8851660]

Goldstein L. Kinesin molecular motors: transport pathways, receptors, and human disease. Proc Natl Acad Sci USA. 2001; 98:6999–7003. [PubMed: 11416178]

Goldstein DJ, Weller SK. Factor (s) present in herpes simplex virus type 1-infected cells can compensate for the loss of the large subunit of the viral ribonucleotide reductase: characterization of an ICP6 deletion mutant. Virology. 1988; 166:41–51. [PubMed: 2842955]

Goldstein LS, Yang Z. Microtubule-based transport systems in neurons: the roles of kinesins and dyneins. Annu Rev Neurosci. 2000; 23:39–71. [PubMed: 10845058]

Grant WB, Campbell A, Itzhaki RF, Savory J. The significance of environmental factors in the etiology of Alzheimer's disease. J Alzheimers Dis. 2002; 4:179–189. [PubMed: 12226537]

Granzow H, Klupp BG, Fuchs Veits W, Osterrieder J, Mettenleiter NTC. Egress of alphaherpes viruses: comparative ultrastructural study. J Virol. 2001; 75:3675–3684. [PubMed: 11264357]

Gunawardena S, Goldstein LS. Disruption of axonal transport and neuronal viability by amyloid precursor protein mutations in Drosophila. Neuron. 2001; 32(3):389–401. [PubMed: 11709151]

Haarr L, Skulstad S. The herpes simplex virus type 1 particle: structure and molecular functions. Apmis. 1994; 102:321–346. [PubMed: 8024735]

Heine JW, Honess RW, Cassai E, Roizman B. Proteins specified by herpes simplex virus. XII The virion polypeptides of type 1 strains. J Virol. 1974; 14:640–651. [PubMed: 4369085]

Hemling N, Roytta M, Rinne J, Pollanen P, Broberg E, Tapio V, Vahlberg T, Hukkanen V. Herpesviruses in brains in Alzheimer's and Parkinson's diseases. Ann Neurol. 2003; 54:267–271. [PubMed: 12891684]

Holland DJ, Miranda-Saksena M, Boadle RA, Armati P, Cunningham AL. Anterograde transport of herpes simplex virus proteins in axons of peripheral human fetal neurons: an immunoelectron microscopy study. J Virol. 1999; 73:8503–8511. [PubMed: 10482603]

Holtzman DM, Bales KR, Tenkova T, Fagan AM, Parsadanian M, Sartorius LJ, Mackey B, Olney J, McKeel D, Wozniak D, et al. Apolipoprotein E isoform-dependent amyloid deposition and neuritic degeneration in a mouse model of Alzheimer's disease. Proc Natl Acad Sci USA. 2000; 97:2892–2897. [PubMed: 10694577]

Huemer HP, Menzel HJ, Potratz D, Brake B, Falke D, Utermann G, Dierich MP. Herpes simplex virus binds to human serum lipoprotein. Intervirology. 1988; 29:68–76. [PubMed: 2842273]

Itzhaki RF, Dobson CB. Alzheimer's disease and herpes. CMAJ. 2002; 167:13. [PubMed: 12137067]

Itzhaki RF, Lin WR, Shang D, Wilcock GK, Faragher B, Jamieson GA. Herpes simplex virus type 1 in brain and risk of Alzheimer's disease. Lancet. 1997; 349:241–244. [PubMed: 9014911]

Jamieson GA, Maitland NJ, Wilcock GK, Craske J, Itzhaki RF. Latent herpes simplex virus type 1 in normal and Alzheimer's disease brains. J Med Virol. 1991; 33:224–227. [PubMed: 1649907]

Jensen HL, Norrild B. Temporal morphogenesis of herpes simplex virus type 1-infected and brefeldin A-treated human fibroblasts. Mol Med. 2002; 8:210–224. [PubMed: 12149570]

Johnson DC, Spear PG. Monensin inhibits the processing of herpes simplex virus glycoproteins, their transport to the cell surface, and the egress of virions from infected cells. J Virol. 1982; 43:1102–1112. [PubMed: 6292453]

Kaether C, Skehel P, Dotti CG. Axonal membrane proteins are transported in distinct carriers: a two-color video microscopy study in cultured hippocampal neurons. Mol Biol Cell. 2000; 11:1213–1224. [PubMed: 10749925]

Kamal A, Almenar-Queralt A, LeBlanc JF, Roberts EA, Goldstein LS. Kinesin-mediated axonal transport of a membrane compartment containing beta-secretase and presenilin-1 requires APP. Nature. 2001; 414:643–648. [PubMed: 11740561]

Kamal A, Goldstein LS. Principles of cargo attachment to cytoplasmic motor proteins. Curr Opin Cell Biol. 2002; 14:63–68. [PubMed: 11792546]

Kamal A, Stokin GB, Yang Z, Xia CH, Goldstein LS. Axonal transport of amyloid precursor protein is mediated by direct binding to the kinesin light chain subunit of kinesin-I. Neuron. 2000; 28:449–459. [PubMed: 11144355]

Klopfenstein DR, Tomishige M, Stuurman N, Vale RD. Role of phosphatidylinositol (4,5) bisphosphate organization in membrane transport by the Unc104 kinesin motor. Cell. 2002; 109:347–358. [PubMed: 12015984]

Koga J, Chatterjee S, Whitley RJ, Jensen HL, Norrild B. Studies on herpes simplex virus type 1 glycoproteins using monoclonal antibodies. Virology. 1986; 151:385–389. [PubMed: 3010559]

Kounnas MZ, Moir RD, Rebeck GW, Bush AI, Argraves WS, Tanzi RE, Hyman BT, Strickland DK. LDL receptor-related protein, a multifunctional ApoE receptor, binds secreted beta-amyloid precursor protein and mediates its degradation. Cell. 1995; 82:331–340. [PubMed: 7543026]

Kristensson K, Lycke E, Roytta M, Svennerholm B, Vahlne A. Neuritic transport of herpes simplex virus in rat sensory neurons in vitro. Effects of substances interacting with microtubular function and axonal flow [nocodazole, taxol and erythro-9–3-(2-hydroxynonyl) adenine]. J Gen Virol. 1986; 67:2023–2028. [PubMed: 2427647]

Kuznetsov SA, Langford GM, Weiss DG. Actin-dependent organelle movement in squid axoplasm. Nature. 1992; 356:722–725. [PubMed: 1570018]

Langford GM, Kuznetsov SA, Johnson D, Cohen DL, Weiss DG. Movement of axoplasmic organelles on actin filaments assembled on acrosomal processes: evidence for a barbed-end-directed organelle motor. J Cell Sci. 1994; 107:2291–2298. [PubMed: 7527056]

Lasek RJ, Brady ST. Attachment of transported vesicles to microtubules in axoplasm is facilitated by AMP-PNP. Nature. 1985; 316:645–647. [PubMed: 4033761]

van Leeuwen H, Elliott G, O'Hare P. Evidence of a role for nonmuscle myosin II in herpes simplex virus type 1 egress. J Virol. 2002; 76:3471–3481. [PubMed: 11884571]

Lo AC, Thinakaran G, Slunt HH, Sisodia SS. Metabolism of the amyloid precursor-like protein 2 in MDCK cells. Polarized trafficking occurs independent of the chondroitin sulfate glycosaminoglycan chain. J Biol Chem. 1995; 270:12641–12645. [PubMed: 7759513]

Lycke E, Kristensson K, Svennerholm B, Vahlne A, Ziegler R. Uptake and transport of herpes simplex virus in neurites of rat dorsal root ganglia cells in culture. J Gen Virol. 1984; 65:55–64. [PubMed: 6319574]

Martenson C, Stone K, Reedy M, Sheetz M, Whealy ME, Robbins AK, Tufaro F, Enquist LW. Fast axonal transport is required for growth cone advance. Nature. 1993; 366:66–69. [PubMed: 7694151]

Matsuda S, Yasukawa T, Homma Y, Ito Y, Niikura T, Hiraki T, Hirai S, Ohno S, Kita Y, Kawasumi M, et al. c-Jun N-terminal kinase (JNK)-interacting protein-1b/islet-brain-1 scaffolds Alzheimer's amyloid precursor protein with JNK. J Neurosci. 2001; 21:6597–6607. [PubMed: 11517249]

McMillan TN, Johnson DC. Cytoplasmic domain of herpes simplex virus gE causes accumulation in the trans-Golgi network, a site of virus envelopment and sorting of virions to cell junctions. J Virol. 2001; 75:1928–1940. [PubMed: 11160692]

Mettenleiter TC. Herpesvirus assembly and egress. J Virol. 2002; 76:1537–1547. [PubMed: 11799148]

Miki H, Setou M, Kaneshiro K, Hirokawa N. All kinesin superfamily protein, KIF, genes in mouse and human. Proc Natl Acad Sci USA. 2001; 98:7004–7011. [PubMed: 11416179]

Miranda-Saksena M, Armati P, Boadle RA, Holland DJ, Cunningham AL. Anterograde transport of herpes simplex virus type 1 in cultured, dissociated human and rat dorsal root ganglion neurons. J Virol. 2000; 74:1827–1839. [PubMed: 10644356]

Molyneaux BJ, Langford GM. Characterization of antibodies to the head and tail domains of squid brain myosin V. Biol Bull. 1997; 193:222–223. [PubMed: 9390390]

Molyneaux BJ, Mulcahey MK, Stafford P, Langford GM. Sequence and phylogenetic analysis of squid myosin-V: a vesicle motor in nerve cells. Cell Motil Cytoskel. 2000; 46:108–115.

Morris RL, Hollenbeck PJ. The regulation of bidirectional mitochondrial transport is coordinated with axonal outgrowth. J Cell Sci. 1993; 104:917–927. [PubMed: 8314882]

Nakajima K, Takei Y, Tanaka Y, Nakagawa T, Nakata T, Noda Y, Setou M, Hirokawa N, Wall JS, Brown JC. Molecular motor KIF1C is not essential for mouse survival and motor-dependent retrograde Golgi apparatus-to-endoplasmic reticulum transport. Mol Cell Biol. 2002; 22:866–873. [PubMed: 11784862]

Neve RL, McPhie DL, Chen Y. Alzheimer's disease: a dysfunction of the amyloid precursor protein (1). Brain Res. 2000; 886:54–66. [PubMed: 11119687]

Newcomb WW, Trus BL, Booy FP, Steven AC, Wall JS, Brown JC. Structure of the herpes simplex virus capsid. Molecular composition of the pentons and the triplexes. J Mol Biol. 1993; 232:499–511. [PubMed: 8393939]

Niclas J, Navone F, Hom-Booher N, Vale RD. Cloning and localization of a conventional kinesin motor expressed exclusively in neurons. Neuron. 1994; 12:1059–1072. [PubMed: 7514426]

Pant HC, Shecket G, Gainer H, Lasek RJ. Neurofilament protein is phosphorylated in the squid giant axon. J Cell Biol. 1978; 78:R23–R27. [PubMed: 690167]

Pietrzik CU, Busse T, Merriam DE, Weggen S, Koo EH. The cytoplasmic domain of the LDL receptor-related protein regulates multiple steps in APP processing. EMBO J. 2002; 21:5691–5700. [PubMed: 12411487]

Prescott AR, Lucocq JM, James J, Lister JM, Ponnambalam S. Distinct compartmentalization of TGN46 and beta 1,4-galactosyltransferase in HeLa cells. Eur J Cell Biol. 1997; 72:238–246. [PubMed: 9084986]

Price DL, Sisodia SS, Gandy SE. Amyloid beta amyloidosis in Alzheimer's disease. Curr Opin Neurol. 1995; 8:268–274. [PubMed: 7582041]

Pyles RB. The association of herpes simplex virus and Alzheimer's disease: a potential synthesis of genetic and environmental factors. Herpes. 2001; 8:64–68. [PubMed: 11867022]

Roghi C, Allan VJ, Wall JS, Brown JC. Dynamic association of cytoplasmic dynein heavy chain 1a with the Golgi apparatus and intermediate compartment. J Cell Sci. 1999; 112:4673–4685. [PubMed: 10574715]

Roizman, B.; Knipe, DM. Herpes simplex viruses and their replication. In: Knipe, DM.; Howley, PM., editors. Fields Virology. Philadelphia: Lippincott, Williams & Wilkins; 2001. p. 2399-2459.

Scaduto RC Jr, Grotyohann LW. Measurement of mitochondrial membrane potential using fluorescent rhodamine derivatives. Biophys J. 1999; 76:469–477. [PubMed: 9876159]

Schnapp BJ, Reese TS, Bechtold R. Kinesin is bound with high affinity to squid axon organelles that move to the plus-end of microtubules. J Cell Biol. 1992; 119:389–399. [PubMed: 1400582]

Schnapp BJ, Vale RD, Sheetz MP, Reese TS. Single microtubules from squid axoplasm support bidirectional movement of organelles. Cell. 1985; 40:455–462. [PubMed: 2578325]

Schroer TA, Brady ST, Kelly RB. Fast axonal transport of foreign synaptic vesicles in squid axoplasm. J Cell Biol. 1985; 101:568–572. [PubMed: 3848436]

Selkoe DJ. Alzheimer's disease: genes, proteins, and therapy. Physiol Rev. 2001; 81:741–766. [PubMed: 11274343]

Signor D, Scholey J. Microtubule-based transport along axons, dendrites and axonemes. Essays Biochem. 2000; 35:89–102. [PubMed: 12471892]

Sisodia SS, Price DL. Role of the beta-amyloid protein in Alzheimer's disease. Faseb J. 1995; 9:366–370. [PubMed: 7896005]

Smith GA, Gross SP, Enquist LW. Herpesviruses use bidirectional fast-axonal transport to spread in sensory neurons. Proc Natl Acad Sci USA. 2001; 98:3466–3470. [PubMed: 11248101]

Sodeik B, Ebersold MW, Helenius A. Microtubule-mediated transport of incoming herpes simplex virus 1 capsids to the nucleus. J Cell Biol. 1997; 136:1007–1021. [PubMed: 9060466]

Stannard LM, Fuller AO, Spear PG, Newcomb WW, Trus BL, Booy FP, Steven AC, Wall JS, Brown JC. Herpes simplex virus glycoproteins associated with different morphological entities projecting from the virion envelope. J Gen Virol. 1987; 68:715–725. [PubMed: 3029300]

Tabb JS, Molyneaux BJ, Cohen DL, Kuznetsov SA, Langford GM. Transport of ER vesicles on actin filaments in neurons by myosin V. J Cell Sci. 1998; 111:3221–3234. [PubMed: 9763516]

Tarr PE, Roncarati R, Pelicci G, Pelicci PG, D'Adamio L. Tyrosine phosphorylation of the beta-amyloid precursor protein cytoplasmic tail promotes interaction with Shc. J Biol Chem. 2002; 277:16798–16804. [PubMed: 11877420]

Taru H, Kirino Y, Suzuki T. Differential roles of JIP scaffold proteins in the modulation of amyloid precursor protein metabolism. J Biol Chem. 2002; 277:27567–27574. [PubMed: 12023290]

Terada S, Hirokawa N. Moving on to the cargo problem of microtubule-dependent motors in neurons. Curr Opin Neurobiol. 2000; 10:566–573. [PubMed: 11084318]

Terasaki M, Schmidek A, Galbraith JA, Gallant PE, Reese TS. Transport of cytoskeletal elements in the squid giant axon. Proc Natl Acad Sci USA. 1995; 92:11500–11503. [PubMed: 8524791]

Tomishima MJ, Enquist LW. A conserved alpha-herpesvirus protein necessary for axonal localization of viral membrane proteins. J Cell Biol. 2001; 154:741–752. [PubMed: 11502759]

Topp KS, Meade LB, LaVail JH. Microtubule polarity in the peripheral processes of trigeminal ganglion cells: relevance for the retrograde transport of herpes simplex virus. J Neurosci. 1994; 14:318–325. [PubMed: 8283239]

Vale RD, Reese TS, Sheetz MP. Identification of a novel force-generating protein, kinesin, involved in microtubule-based motility. Cell. 1985a; 42:39–50. [PubMed: 3926325]

Vale RD, Schnapp BJ, Reese TS, Sheetz MP. Movement of organelles along filaments dissociated from the axoplasm of the squid giant axon. Cell. 1985b; 40:449–454. [PubMed: 2578324]

Verhey KJ, Meyer D, Deehan R, Blenis J, Schnapp BJ, Rapoport TA, Margolis B. Cargo of kinesin identified as JIP scaffolding proteins and associated signaling molecules. J Cell Biol. 2001; 152:959–970. [PubMed: 11238452]

Whealy ME, Robbins AK, Tufaro F, Enquist LW. A cellular function is required for pseudorabies virus envelope glycoprotein processing and virus egress. J Virol. 1992; 66:3803–3810. [PubMed: 1316483]

Whitley, RJ. Herpes simplex viruses. In: Knipe, DM.; Howley, PM., editors. Fields Virology. Philadelphia: Lippincott, Williams & Wilkins; 2001. p. 2461-2506.

Willard M. Rapid directional translocations in virus replication. J Virol. 2002; 76:5220–5232. [PubMed: 11967336]

Wollert T, Weiss DG, Gerdes HH, Kuznetsov SA, Wall JS, Brown JC. Activation of myosin V-based motility and F-actin-dependent network formation of endoplasmic reticulum during mitosis. J Cell Biol. 2002; 159:571–577. [PubMed: 12438410]

Xu F, Schillinger J, Sternberg M, Johnson R, Lee F, Nahmias A, Markowitz L. Seroprevalence and coinfection with herpes simplex virus type 1 and type 2 in the United States, 1988–94. J Infect Dis. 2002; 185:1019–1024. [PubMed: 11930310]

Zheng P, Eastman J, Vande Pol S, Pimplikar SW. PAT1, a microtubule-interacting protein, recognizes the basolateral sorting signal of amyloid precursor protein. Proc Natl Acad Sci USA. 1998; 95:14745–14750. [PubMed: 9843960]

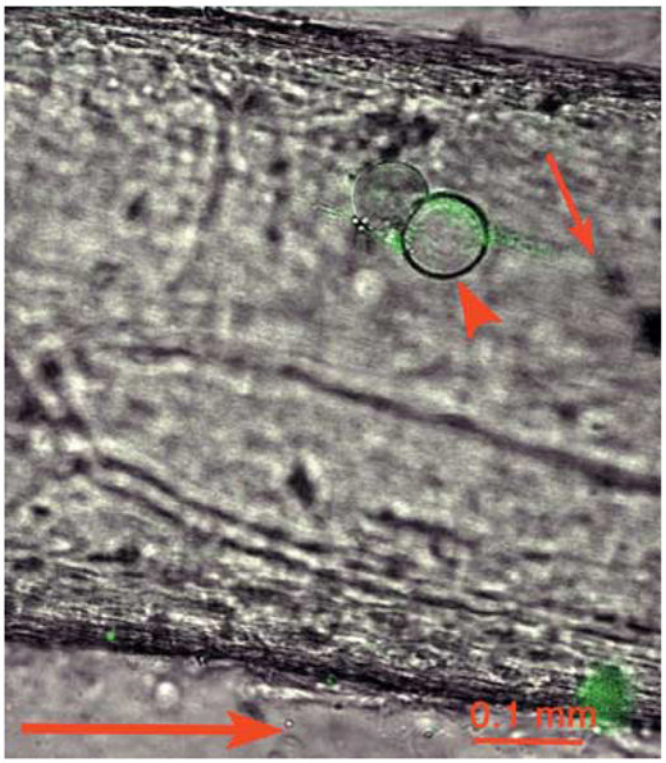

Fig. 1.
VP16-GFP-labelled HSV imaged by confocal microscopy after injection into the squid giant axon. Green GFP-HSV particles form a plume (small arrow) at one side of the oil droplet (arrowhead), which marks the injection site, imaged by dual-channel confocal microscopy with DIC and fluorescein fluorescence. This plume points towards the synapse and away from the cell body (anterograde indicated by large arrow below). Viral particles appear green.

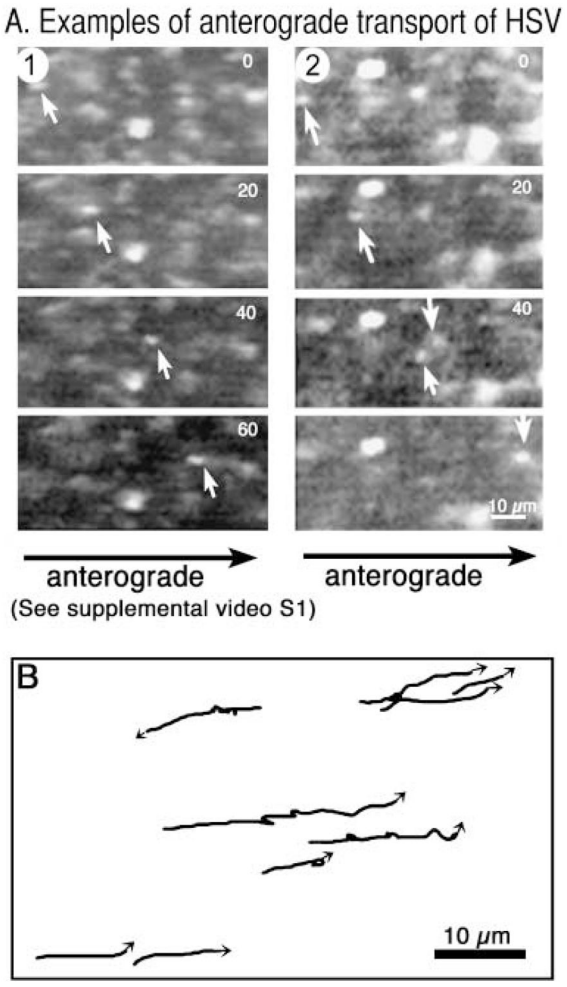

Fig. 2.

Fast anterograde transport of GFP-HSV in the squid giant axon. (A) Video sequence (39 frames, 2.67-s time lapse) of an individual VP16-GFP labelled particle travelling in the anterograde direction after injection into the axon. Adjacent stationary particles testify to the specificity of this movement. Some quenching of the GFP occurs as a result of the large amount of laser power required to obtain images rapidly of these small moving particles. (Please refer to Supplementary Material section for information on how to view the video clip in full.) (B) Tracings of VP16-GFP particle movements from a 50-frame/138-s sequence showing that viral particles may pause up to three times during this time span, some displaying short retrograde movements during pauses. In this field, one particle travels retrograde.

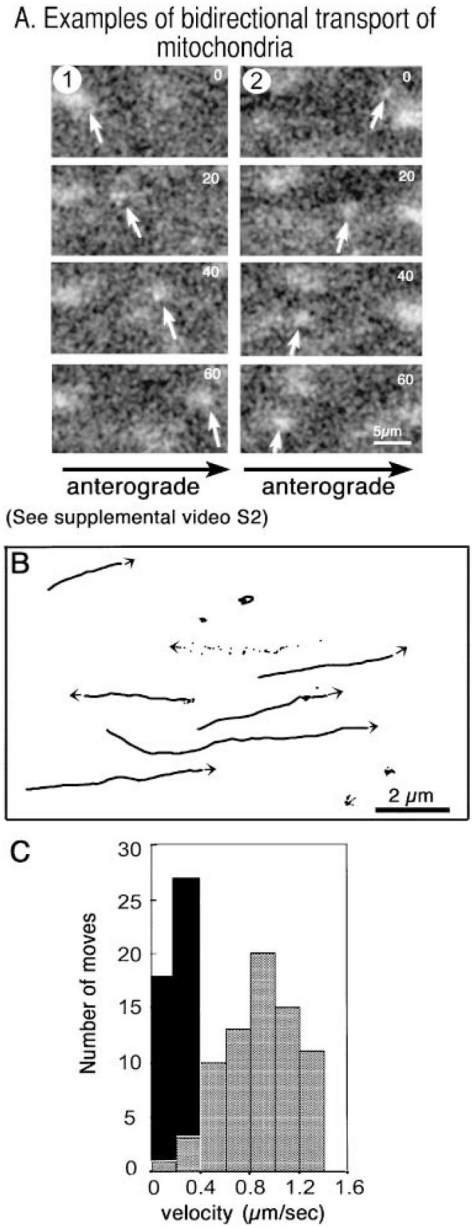

Fig. 3.

Mitochondria travel more slowly than HSV and in both directions. (A) Mitochondria, stained with the cell-permeable mitochondrial dye, R123, and imaged in the same axon as Fig. 2, demonstrate bi-directional movements in video sequences (24 frames, 5-s interval). (Please refer to Supplementary Material section for information on how to view the video clip in full.) (B) Tracings of mitochondrial tracks show frequent pauses, rare reversals and both anterograde and retrograde transport (two of seven move retrograde). One track is shown as a series of dots representing the location of this mitochondria in each of 24 frames, which reveals the saltatory nature of the movements. Note the magnification bar is five- to ten-fold greater than that of the viral movements shown in Fig. 2(B) in the same axon. (C) Histogram comparing velocity ($\mu m\ s^{-1}$) and number of movements for representative viral particles (grey bars, $n = 73$) and mitochondria (black bars, $n = 45$).

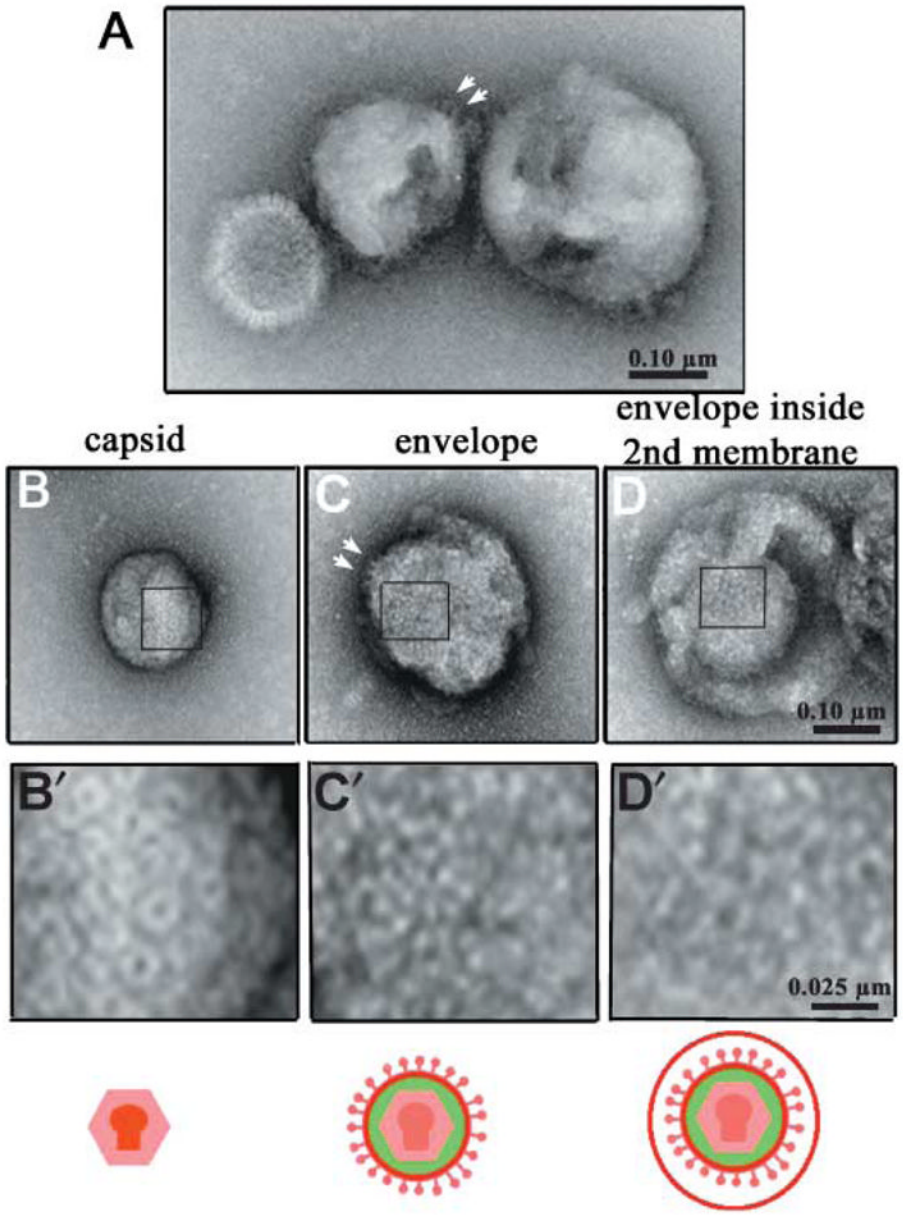

Fig. 4.

Electron microscopy shows enveloped HSV inside a second membrane. (A) Three viral particles displaying each type of morphology present in the motile preparation. From left to right, capsid (130 nm), envelope (230 nm) and larger membranated particle (300 nm). (B–D) Surface texture of representative examples for each type of viral particle. Below each type of particle is a higher magnification image correlating to the area indicated by the rectangle: (B,B′) capsid; (C,C′) envelope; (D,D′) larger membranated particle broken open to display a viral particle within. When envelopes are imaged in silhouette (arrows in A and C), glycoprotein studs are particularly evident. The size of the particle inside the larger membrane (D) and its surface texture (D′) correlates with that of enveloped virus (C,C′) and not with capsid (B′).

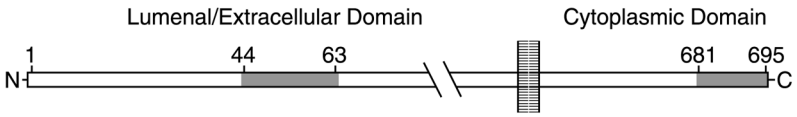

Fig. 5.
Diagram of APP and location of peptides recognized by C-APP and N-APP antibodies.

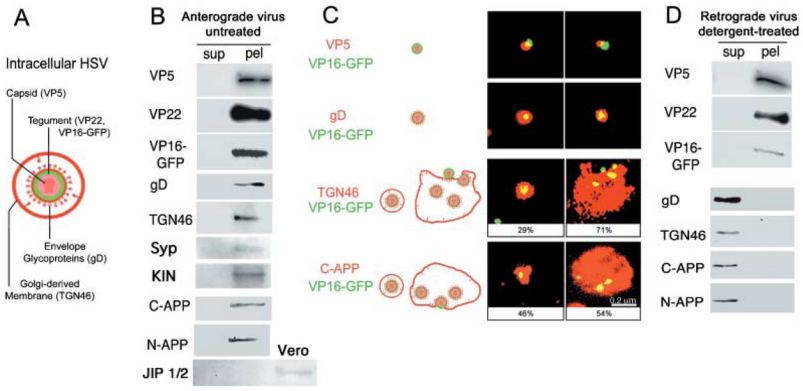

Fig. 6.

APP and TGN46 are associated with motile GFP-labelled HSV. (A) Diagram of HSV indicating the viral and host cell compartments recognized by the antibodies. (B) Cellular proteins co-sediment with GFP-HSV. Motile virus preparations were separated into particulate and soluble proteins by centrifugation and the resultant supernatants (sup) and pellets (pel) probed for proteins representative of each compartment by immunoblotting. Both viral and cellular proteins are detected only in the pellet: viral capsid (VP5), tegument (VP22), envelope (gD) and the VP16-GFP label (GFP), together with TGN46, a *trans*-Golgi marker, and APP detected with two different antibodies, one against the peptide in the cytoplasmic domain, C-APP, and the other against the extracellular domain, N-APP. Both anti-APP antibodies detected a single, ~120-kDa band in the pellet that could be superimposed in stripped and re-probed blots. Synaptophysin and kinesin are also detected in pellets of viral particles. JIP is not detected in either the supernatant or the pellet from the virus, but is present in the Vero cells (additional third lane from left). (C) Immunofluorescence shows that the cellular proteins, TGN46 and APP, are associated with GFP-labelled viral particles. Preparations of motile VP16-GFP-labelled HSV stained for viral compartments, capsid (VP5), envelope (gD), as well as cellular proteins (TGN46 and C-APP). Antibodies appear red, VP16-GFP-labelled HSV is green and overlap appears yellow. The GFP-label was associated with all three viral compartments, demonstrating that labelled particles represent intact virus. Appropriately, capsid (VP5) was within or beside the GFP, and envelope (gD) surrounded GFP label. GFP-labelled particles were also found associated with C-APP and TGN46. C-APP was apparently exposed on the particle surface, as it was detected without fixation or detergent. Both anti-TGN46 and anti-C-APP stain two different structures: small particles containing a single virus and large cisternae with multiple virions. Percentiles indicate the average proportion of each type of structure in motile viral preparations. The scale bar, bottom right, is the same for all images. (D) Detergent treatment which removes anterograde motility also separates APP from labelled viral particles. Motile preparations of GFP-labelled HSV were treated with Triton-X100 under conditions known to deplete anterograde and enhance retrograde motility (Bearer *et al.*, 2000). Supernatants (sup) and pellets (pel) were separated by centrifugation and protein composition analysed by immunoblotting in parallel with untreated virus as shown in (B). Viral particles retained proteins representative of capsid and tegument (VP5, VP22) and the GFP label, whereas membrane components were solubilized (gD, TGN46 and APP). As in (B), APP was detected with two different antibodies, both of which detect a single band in the supernatant.

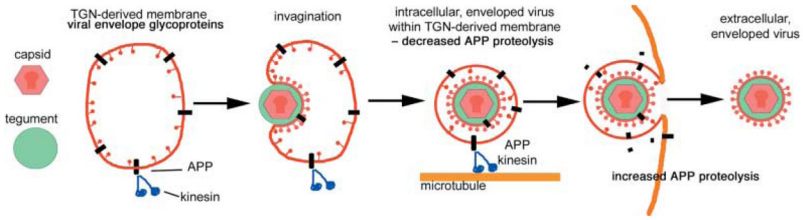

Fig. 7.

Diagram showing how HSV interaction with APP may occur in the cell and the role of this interaction in transport. Viral capsid (red) is assembled in the nucleus and joins the tegument (green) in the cytoplasm. Viral gylcoproteins are synthesized in cellular membrane compartments, and arrive in the Golgi apparatus where APP is also concentrated (black). Viral tegument binds to tails of viral glycoproteins, aggregating them in the plane of the membrane and the capsid joins this assembly. This assemblage of viral components then invaginates or buds into the lumen of Golgi-derived secretory vesicles, acquiring the viral envelope in the process. APP may be passively or actively recruited into the viral envelope as well as remaining in the membrane of the cellular secretory vesicle where it exposes its C-terminus to the cytoplasm. The C-terminus of APP recruits cytoplasmic kinesin from the cytoplasm to the surface of the virus-containing vesicle. Kinesin then motors the vesicle along microtubules down the axon to the synapse. During transit, HSV may protect APP from proteolysis. Exit of the virus releases this protection and proteolysis of APP begins. This scenario could result in increased accumulation of APP at the periphery where toxicity of the proteolytic fragments could underlie pathogenic effects of HSV. Long-term derangement of transport and of location of APP processing may therefore result in neuronal dysfunction and death.

Table 1

Comparison of velocities (μm s^{-1}) of HSV, endogenous organelles, and beads in squid axons

	Average velocity	Maximum velocity
VP16-GFP HSV in squid axon	0.9 ± 0.3 (*n* = 73)	1.23
Mitochondria (anterograde) in squid axon	0.2 ± 0.08 (*n* = 45)	0.36
Uncoated beads in squid axons *	0.078 (*n* = 70)	0.40
Uncoated beads in crab axons †	0.3 (*n* = 22)	0.6
Organelles inside squid axon (0.1–0.2 μm diameter) ‡	0.25	5
Organelles in extruded axoplasm §		
Vesicle diameter:		
< 0.2 μm	2.15	
0.2–0.53 μm	1.1	
> 0.53 μm	0.4	

* This study and Terasaki *et al.* (1995).

† Adams & Bray (1983).

‡ Allen *et al.* (1982), and Vale *et al.* (1985).

§ Vale *et al.* (1985).